E3S Web of Conferences **564**, 09003 (2024) https://doi.org/10.1051/e3sconf/202456409003
ICPGRES-2024

Investigation of maximum power point tracking of different kinds of solar panel under partial shading conditions

Dr.G.R. Vijayshankar[1*], ***K. Dhivya***[2], ***Laeth H.J. Hamza***[3], ***M. Priyadharshini***[4] ***and G.Mallikarjuna Rao***[5]

[1]*Department of Civil Engineering, Karpagam Academy of Higher Education, Coimbatore- 641021*
[2]*Department of Civil Engineering, Karpagam College of Engineering, Coimbatore- 641032*
[3]*Department of Structurals Techniques Engineering, College of Technical Engineering, The Islamic University, Najaf, Iraq; Department of Structurals Techniques Engineering, College of Technical Engineering, The Islamic University of Al Diwaniyah, Al Diwaniyah, Iraq; Department of Structurals Techniques Engineering, College of Technical Engineering, The Islamic University of Babylon, Babylon, Iraq*
[4]*Assistant Professor, Department of CSE(DS), CMR Institute of Technology, Hyderabad*
[5]*Department of CSE, GRIET, Hyderabad, Telangana, India*

Abstract. In order to remove the most outrageous potential result power with high following viability in varied working situations, photovoltaic (PV) systems should operate at a largest power point (MPP). This essay examines yet another insane power point following (MPPT) method for eliminating the pinnacle electricity from the PV board or bunch in situations that are primarily concealed (PSCs). In the suggested calculation, the overall apex (GP) with a high mixing rate and high following efficiency is sought for by the estimation, which takes into account the bio-awakened Whale Upgrade (WO) with reinitialization process when the PV structure is subjected to change in hidden model. The suggested computation lowers the computational burden associated with the current MPPT estimates as stated in different compositions and lessens power stalling when operating conditions vary. The suggested method is demonstrated and replicated using MATLAB/Simulink programming in several test scenarios. The suggested procedure is carried out in a distinct and regular manner, aggravating and providing insight (PO). The following time and following capacity of the Dull Wolf Improvement (GWO) and Creamer GWO (HGWO) approaches, as well as the diversion outcome, demonstrate that the WO technique has a high following efficiency (>95%) and a short mixing time (<0.15sec) under PSCs with less power movements. The execution assessment is completed in a similar manner to the fill portion, relative effect disaster/gain, and dumbfounding mishap.

1 Introduction

Soon after, the maintainable power source was developed quickly with the idea that it would provide ideal and efficient power energy. The sun-positioned photovoltaic system (PV) anticipates a significant portion of the vast array of sustainable power sources to

* Corresponding author: gmprojects@karpagam.com

 https://doi.org/10.1051/e3sconf/202456409003

generate pollution-free energy by converting solar energy into electrical energy produced by MPPT methods in order to remove the high output power from the PV board. The main goal of determining the MPP is to coordinate the converter's output power in order to normalize the PV module's operating voltage. By altering the converter commitment cycle, this is achievable. The commitment cycle is adjusted in accordance with finding the PV module's P-V characteristic's optimal operating point. As such, a crucial component of all PV systems is the MPPT control (Belhachat and Larbes, 2019; Premkumar et al., 2018; Premkumar and Sowmya, 2019; Riaz et al., 2019; Abdul-Kalaam et al., 2016) [1]. The authors of El-Khozondar et al. (2016), Sutikno et al. (2014), and Haidar et al. (2018) examined several MPPT systems for PV constructions.

An organized review of various MPPT systems, including standard strategies (consistent conductance (IC) and trouble and insight (PO)), halfway open/cut off/current systems, and significant level MPPT techniques (taking differential turn of events (Kok Soon et al., 2014) into consideration), was provided by the creators of Karami et al. (2017), feathery reasoning control (FLC) (Ahmad El et al., 2014, etc.), atom swarm smoothing out (PSO) (Yi-Hwa et al., 2012), and (ANN) (SantiAgatino and Giacomo, 2015). The most popular MPPT techniques are PO and IC, which have a few benefits such a simple structure, low cost, easy implementation, and minimal limitations evaluation (Premkumar&Sumithira, 2019) [2]. Regardless, these processes fail to identify the MPP in the rapidly approaching normal situation. These estimates lead to increased influence mishap and settle at a nearby zenith (LP). The limitations of the conventional calculations are surpassed by current MPPT methods like dull wolf smoothing out (GWO) (Mohanty et al., 2016), cuckoo search (Peng et al., 2018), fireflies (Sundareswaran et al., 2014), Jaya estimation (Huang et al., 2018), differential progression (Kok Soon et al., 2014), innate estimation (Badis et al., 2017), fake bumble bee territory (Benyoucefa et al., 2015), ANN (SantiAgatino and Giacomo, 2015), and FLC (Ahmad El et al., 2014). These calculations are known as metaheuristic estimates, and they have the benefit that it is possible to look at the request space (such as the P-V brand name) more thoroughly and, as a result, control the In any case, it is set up according to speed of follow, and these systems are much slower than their traditional counterparts (Ahmed and Salam, 2015; Kermadi and Berkouk, 2017). In order to further increase the rate of collection,

The researchers provide the modified calculations for handling fragile objects. The authors of Ji-Ying et al. (2016) suggested a modified cuckoo search approach that eliminates the unpredictable nature of the traditional cuckoo search method. In general, the blend speed research is known from computations such as crossbreed GWO (Mohanty et al., 2017), blend WO (Premkumar and Sumithira, 2018), hybrid FLC (Bahrami et al., 2016), cross variety ANN (Jiang et al., 2015), blend Jaya (Chao et al., 2019), cross variety PSO (Farh et al., 2018), etc [3].

In order to acquire high following capability under a rapid likewise, foolish change in sun-based brightness, the creator of Mohanty et al. (2017) connects the GWO and PO. The PO takes into account the final step to attain the high blend rate, whereas the GWO takes into account the fundamental GP [4]. In order to understand the unparalleled following speed with high following capacity under varied working situations, the WO and PO are combined to reduce the calculation time. According to Premkumar and Sumithira (2018), the WO locates the concealed GP, and the PO completes the last step to obtain a high mix rate. The proposal of Jiang et al. (2015) is to combine the ANN and PO to appear at a quicker mix rate. Initially, the ANN locates the GP; as a result, PO controls the converter's commitment example to determine the apex working point. In Chao et al. (2019), the Gaussian process backslide is combined with Jaya computation for PV bunch under PSCs. In any case, the computational discomfort surpasses that of the self-governing MPPT systems.

In light of the problems with the traditional and modern MPPT techniques—such as low following efficiency, low following accuracy, high blend time, and high estimation weight—this paper suggests a different free WO MPPT system that combines features—like reinitialization—that lead to performance enhancement [5]. Due to the inspection, abuse restriction, and ability to dismiss the LPs, the WO calculation has a greater relevance than other estimates. By reducing the number of search experts, the suggested computation's search time is shortened without sacrificing accuracy. Reduce the number of search specialists significantly to speed up the association time. Furthermore, during the dependable stage, power influencing is smaller, and the estimation approaches the MPP rapidly. In essence, the suggested method may be ready to produce a rapid and robust GP following; reliable gathering in insufficient covering conditions that unifies the P-V brand name with different zeniths. The following is how the document is facilitated. The PV module display and the attributes under partial covering situation are shown in Portion 2.

Additionally, Region 3 provides an overview of the proposed estimation's architecture and explains how WE computation with reinitialization is applied to MPPT applications. The propagation findings and other debates are analyzed in Part 4. The presentation of the suggested MPPT system is examined in Part 5 to the degree that relative impact adversity/gain, fill factor, and bewildering hardship are present. The publication eventually closes in Portion 6.

2 Sun based PV credits under various working conditions

For the PV board, the normal current (I)-voltage (V) relationship is not linear. As a result, it is crucial to consider this as the best starting point for eliminating the most absurd outcome power. In any case, when the temperature changes in addition to the daylight-based brightening, the PV module's yield power varies [6]. Work on the PV board at MPP is essential, as demonstrated by the financial working area action (Madeti and Singh, 2017). When the load resistance and the module deterrence are the same, the module produces the most astonishing amount of energy. By adjusting the dc converter's commitment extent, the traditional dc converter is connected between the module and the store to meet the load security provided by the internal board resistance.

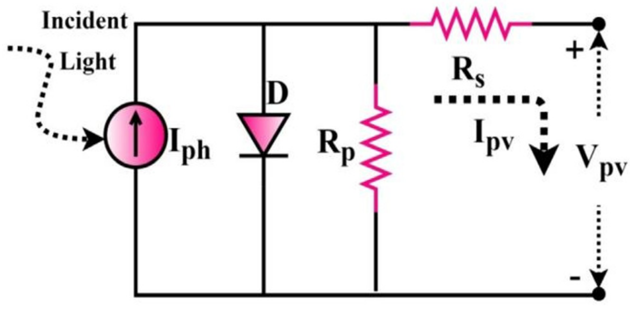

Fig. 1. Shows the PV module's indistinguishable circuit when using the one diode model

2.1 A representation of the solar-powered PV board

The single diode model displays the PV module,

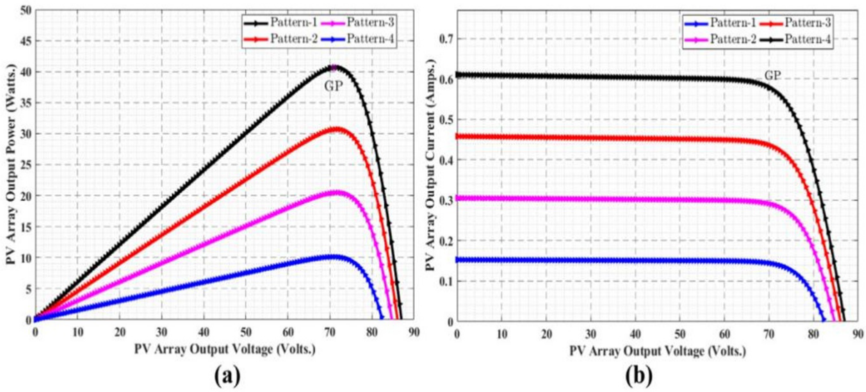

Fig. 2. Shows the characteristics of a PV array under uniform illumination: the P–V characteristic and the V–I characteristic

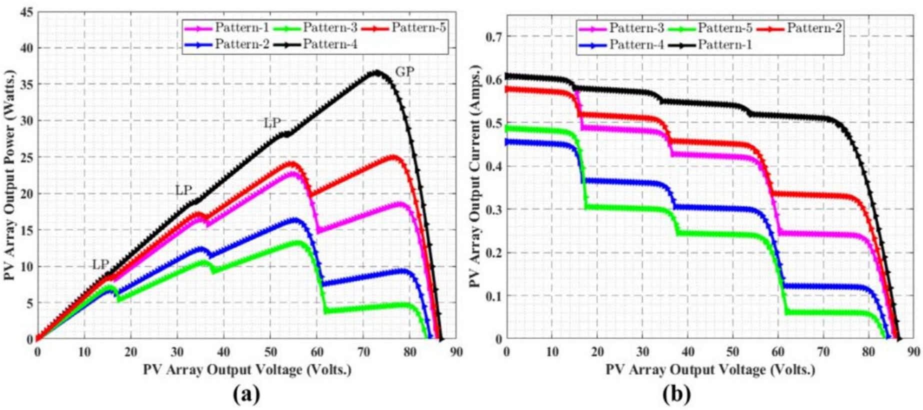

Fig. 3. PV array properties under photovoltaic cells (PSCs): (a) PV array characteristics, (b) V-I characteristics

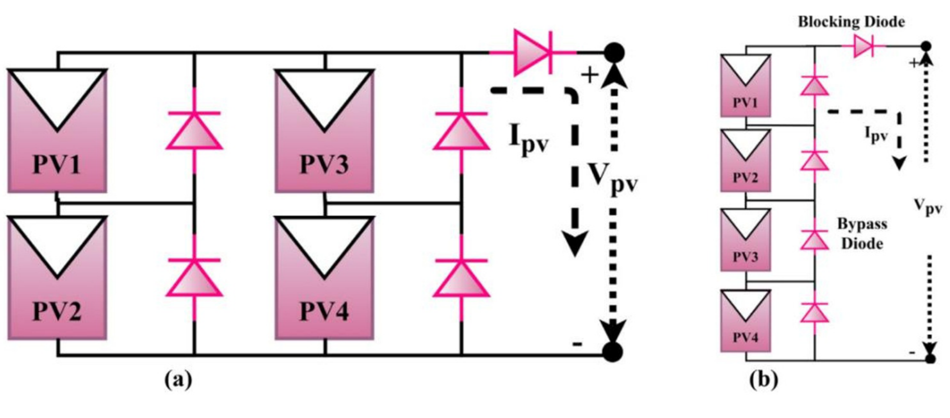

Fig. 4. PV array topologies are shown in (a) and (b) as 2S2P (series-parallel) and 4S, respectively

2.2 The impact of largely covered conditions on photovoltaic displays relying on daylight

The PV bunch is assembled socially, with the PV modules in series and equal mixes. Recognizing that the PV module is abused by PSCs, it draws more power and promotes the PV cell's forced convergence. This creates the difficulty spot, which is then generally reduced by partnering the diversion diode across the photovoltaic module. It is important to examine the PV module, string, or bunch's characteristics under both uniform and non-uniform operating situations since the presence of the diversion diode causes variations in the board's quality during PSCs (Priti et al., 2017). The PV cell's output voltage must satisfy the criterion stated in Equation (6) under partially covered conditions, and the diversion diode begins coordinating at that point [7].

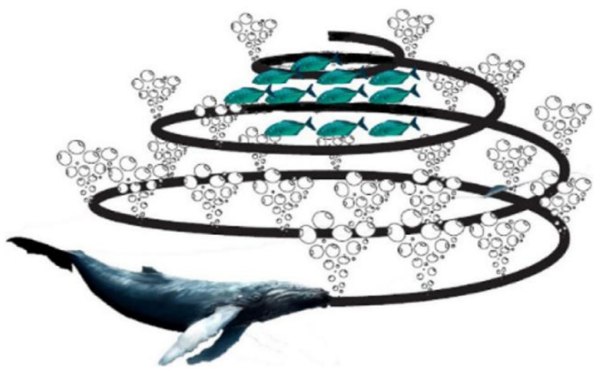

Fig. 5. Instrument for searching for bubble-net feed (Mirjalili and Lewis, 2016)

whereVd,on tends to the diode's forward on-state voltage. As was previously said, in light of the elude diode's conduction, several apexes, such as distinct LPs and a single GP under PSCs, occur. The module's output current is obviously comparable and is dependent on light from the sun. As a result, the solar light detects the PV module short out current [8].

Similar to this, the PV module's output voltage is relative and contingent upon the temperature of the cell. In any event, the PV yield current is also created by temperature increases. This means that low PV yield power is achieved when there is a drop in yield voltage due to a high cell temperature. The sun-based PV group configurations are depicted in Fig. 4 as two series-related strings with two comparable ways (2S2P) and four series-related modules (4S). Fig. 4 shows that in order to shield the bunch from the switch current, the PV group is supplied one hindrance diode and diversion diodes across each board. The greatest functioning attribute of the PV module is evolving consistently throughout the day due to the constant changes in temperature and sun-based insolation. If the functional point is not near the MPP, the influence incidence may be high. Finding the MPP is therefore crucial, and this may be done by applying a reasonable MPPT technique [9].

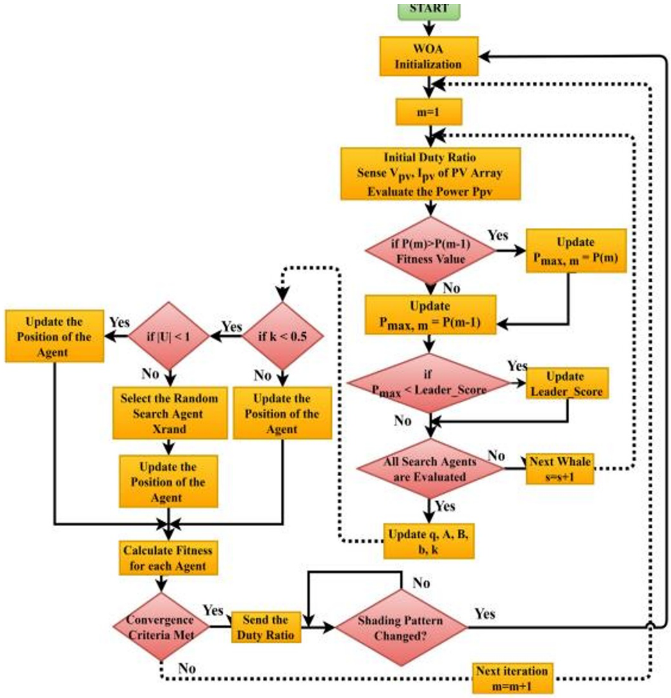

Fig. 6. A flowchart showing the reinitialization procedure and the suggested WO MPPT approach

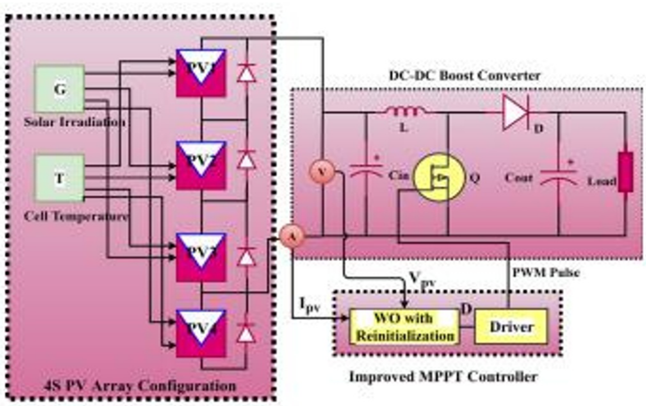

Fig. 7. Block schematic of the solar-powered PV construction using the WO MPPT technology

3 The suggested WO MPPT method's blueprint, which includes reinitialization

3.1 Fundamental ideas for estimating whale smoothing

One of the smart bio inspired estimates is the whale smoothing out computation, which is supported by the whale's hunting activities. This lead may be utilized to address non-straight concerns in planning, as humpback whales are quite prevalent in hunting. The term "hunting" refers to the use of bubble-net feed, and Fig. 5 (Mirjalili and Lewis, 2016) shows a comparison. These whales hunt for the little fish that are close to the surface. The search begins with the air pockets in the roundabout and continues with the goal, bubble-net feed, and goal searches in the areas of abuse and examination [10]. The pursuit specialist locates the objective location and closes in on the target. The estimator predicts the evenhanded as the continuous best course of action because of the dark fundamental request space position, and it locates the best whale while doing different tasks to keep things moving forward. Within the contracting circle, the experts swim near the target prey and adjust the optimal location. 3.2. Using the WO MPPT method. The suggested WO MPPT approach aims to identify the GP with low power faltering and high following efficiency under a variety of working settings, such as uniform and nonuniform illumination. In order to reduce the power influencing the commitment cycle, WO is used in this research as a prompt control MPPT approach. This involves assuming the role of the energizing chase specialist. This prompt management technique reduces impact setback and, as a result, increases viability. The best expert's standing is restored as search experts become closer to one another. The suggested MPPT technique's flowchart is displayed in Fig. 6, and the following is a description of the execution process [11].

Stage 1: Within 20% (dmin) to 92% (dmax) of the typical DC converter commitment cycle, the search expert position is established.

Stage 2: To create the PV bunch yield power and recalculate the power by managing the PV voltage and current at each commitment cycle, the converter is driven at every optimal location selected by the chase expert.

Step 3: The pursuing subject matter expert's position is altered by the objective's capability to intensify the result, as shown by the converter's commitment example in Equation (11).

Stage 4: Repeat steps 3–4 until all request-trained personnel have complied with the mix/end standards. Eq. (13) presents the final rule. Using Eq. (13), the suggested WO calculation is reinitialized by addressing the change in yield power. When the PV structure is exposed to a change in the disguise plan, the WO estimate is reinitialized. With this collaboration in reinitialization, the PV structure becomes the ultimate follower of the GP. The calculation provides good following adequacy and tracks down the GP with a little smaller step size to reduce power faltering [12].

In order to obtain the best attention, the exploratory setting is necessary. For instance, inconsistent numbers are used to alter the request expert's maltreatment and examination duration, eroding the likelihood of receiving the GP. A few studies addressed the guarantee of optimal value (Ahmed and Salam, 2015; Kermadi and Berkouk, 2017). To determine the potential result of the computation, a number of tests are conducted. Since one-layered ability (single objective capacity) was covered in this study, determining limitations is simple. By altering the blending precision and estimate duration, the request experts are constrained [13]. The boundaries are chosen with the talks from Kermadi and Berkouk (2017) and Ahmed and Salam (2015) in mind for the reenactment emphasis on in this The vector location of the best request expert to eliminate the usage of the PID controller provides the commitment example for the DC converter. Fig. 7 displays the block diagram of the solar-positioned PV system using the suggested MPPT technique. Variations in the concealment models cause the PV module/bunch's output power to fluctuate. The estimator is reinitialized by examining the power faltering, as was previously mentioned. Selecting infinite pursuit-trained specialists increases following accuracy; nonetheless, computation unpredictability and following time are increased [14]. This research considers the movement of the input variable with different consistent constraints and notes the impact on the objective ability. The goal of the WO calculation is to locate the optimum position in both chase spaces in order to determine the overall optimal game strategy. The limitations are chosen after a focused assessment and several starting running. In this article, twelve request experts are selected in order to minimize the complexity of the estimating process without sacrificing accuracy.

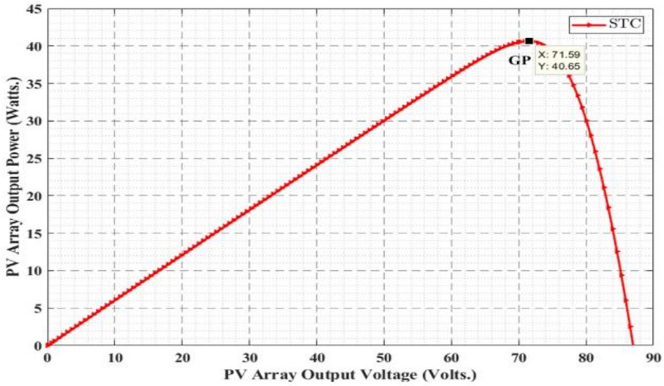

Fig. 8. PV group's P-V characteristic under STCs

4 Discussions and outcomes from the reenactment

MATLAB/Simulink programming is used to display the suggested estimation, and the PV system was used for the reenactment under various studies, including STC, PSCs, and sudden and drastic changes in insolation. The limitations of each PV module individually include

Figure 9 shows the generation waveforms at STCs: PV group yield current, PV show yield power, PV show yield voltage, and PV commitment cycle as follows [15]: Manufacturer: Andslite Daylight-based charger; features include Pmpp = 10.16 W, Vmpp = 17.83 V, Impp = 0.57 A, Voc = 21.75 V, and Isc = 0.61 A. The accompanying lists the following details about the lift converter's subtleties: trading repeat (Fsw) of 20 kHz; yield voltage range (Vout) of 120-300 V; input voltage range (Vin) of 40-100 V; inductance (Ldc) of 4.17 mH; input capacitor (Cin) of 220 µF; and most outrageous power (Pmax) of 100 W. It is determined to support the inclusion of the suggested approach in the 4S PV bunch plan.

This document does not include the additional bunch designs, such as honeycomb, series-equivalent, full cross tied, and length association. In any case, the suggested method may work for other PV bunch geologies [16].

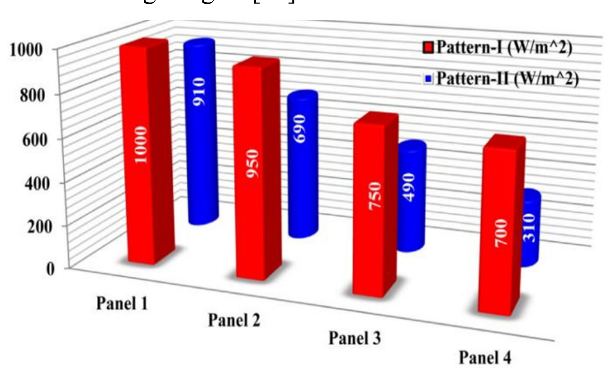

Fig. 9. Various covering models that were shown for the first defense

4.1 Examine I:STCs

The suggested technique's introduction was completed in accordance with STCs at every stage. An industrial standard known as the STC determines the PV module's operating temperature, which is set at 25 ◦C for the cell, 1000 W/m^2 for the sun's radiation, and 1.5 ranges for the air mass. In any case, it is rare that the requirements for STC are satisfied. The PV display brand name (P-V) is displayed in Fig. 8, and various result limits—such as the PV display yield voltage, yield current, yield power, and commitment cycle under STCs—are displayed in Fig. 9.

The WO MPPT approach may be developed to track the MPP of the bunch, for example, 40.53 W out of 40.65 W at STCs, as Fig. 9(a) illustrates. By comparing the outcomes to the usual PO, GWO, and HGWO estimations, the WO technique's introduction is validated. The PO estimate can be ready to track 40.52 W, the GWO computation can follow 40.51 W, and the HGWO computation can follow 40.53 W [17]. It is evident that there is some hesitancy in the PO method, which can generally be minimized by selecting a more modest step size. However, doing so would lengthen the association time. The subsequent times for WO, PO, GWO, and HGWO are, respectively, 0.1246 s, 0.1515 s, 0.1248 s, and 0.1285 s. With varying follow-up times, all calculations may be built to monitor essentially the same MPP under STCs. It is believed that modern MPPT approaches, such as WO, GWO, and HGWO, perform better in STCs and exhibit nearly equivalent features to the traditional PO estimate. The PV group yield voltage and current are supporting waveforms that truly take a look at the PV structure, as seen in Fig. 9(b)–(c).

The commitment cycle shift under STCs is seen in Fig. 9(d). The ideal commitment examples for WO, PO, GWO, and HGWO are seen to be, respectively, 0.3263, 0.4485, 0.3263, and 0.3111 during the calculations' basic time [18].

4.2 Examine II: PSCs

To locate the GP rather than the LPs, the PV system using the suggested WO MPPT approach is supported under PSCs. The PV group that faces the sun is used to create the covering models, as seen in Fig. 9. Fig. 10 displays the P-V quality of a 4S PV group arrangement under PSCs (for two distinct covering models). The P-V brand name contains three LPs and one GP under both model I and model II, as seen in Fig. 11. The by-pass diode perceives the local tops as normal. The converter's primary commitment is commitment cycle acclimation, which may fluctuate depending on the PV group yield voltage and PV group yield current in order to obtain the most extravagant power situation under PSCs [19]. Because of the restricted step size, the PO estimation attempts to settle at third nearby top during the MPP request duration but is unable to appear at the GP. Many parameters of PV, partial shading and converter as well as modelling are considered from [30-39].

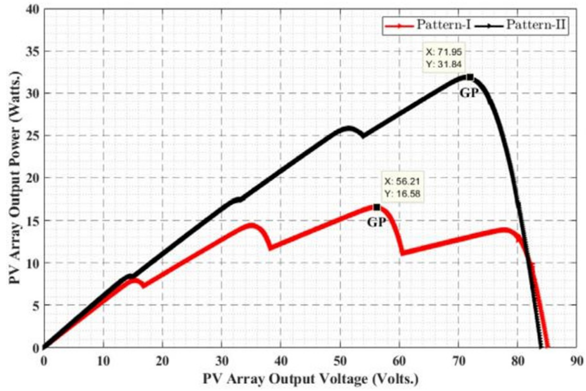

Fig. 10. PV group's P-V property under PSCs

Two coverage models constructed at 0.25 s length are presented in Fig. 10 to support the estimation. LP1 at 7.8 W, LP2 at 14.58 W, LP3 at 13.22 W, and one GP at 16.5 W are only a few of the LPs associated with the P-V brand name at plan I, as seen in Fig. 11. Similarly, LP1 at 8.2 W, LP2 at 17.38 W, LP3 at 26.66 W, and one GP at 31.84 W are among the LPs associated with the P-V brand name at plan II.

Plan II is created at t = 0.25 s, while model I is made at t = 0, as seen in Fig. 12(a). Plan I allows the PV system with the WO calculation to be set up to follow the best power of 15.97 W at t = 0.1297 s. Examining the trial results provided by the GWO, HGWO, and traditional PO estimations supports the implementation of the WO computation. The GWO computation may be ready to go after 14.26 W, the PO estimation can be ready to go after 13.12 W, and the HGWO estimation can be ready to go after 14.88 W. PO, GWO, and HGWO have associated times of 0.1620 s, 0.1537 s, and 0.1328 s, respectively. Under plan II, the PV system with the WO estimate may be set up to follow the best power of 30.41 W at t = 0.1849 s. The PO estimate can be ready to go along with W23.13, the GWO estimate can go along with W28.38, and the HGWO estimate may go along with W 29.12. PO, GWO, and HGWO have associated times of 0.2147 s, 0.1957 s, and 0.1798 s, respectively. The PV display yield voltage and current are supporting waveforms, which validates the PV system's presentation. The commitment cycle change under PSCs is seen in Fig. 12(d). The optimal commitment examples for WO, PO, GWO, and HGWO are seen to be, respectively, 0.2639, 0.4485, 0.3165, and 0.2445 at the Multiplication waveforms at PSCs: PV Power Yield, PV Voltage Yield, PV Current Yield, and PV Commitment Cycle. As can be observed, the collecting time for the standard PO calculation is longer than the suggested WO computation, and it attempts to follow the GP under PSCs. Since it reinstates the position of the chase trained professional in a single setup, the other estimates, such as GWO and HGWO, lack an uncommon overseer to isolate explicit accentuation to the maltreatment or the examination search space. As a result, the probability of falling into LP is more legitimately extended in these computations. Given the hybridization, the PO's path close to the GP will cause the HGWO to follow the most outrageous power, which is about equivalent to the WO estimate. The WO computation is inferred to attempt to settle much closer to the GP in light of the whales' revival and unconditional reinitialization in both arrangements to further enhance the gathering accuracy.

4.3 Test III: Quick shift in illumination dependent on the sun

After a brief shift in insolation, the PV structure with the suggested WO MPPT approach is approved in order to determine the GP accounting for all of the LPs.The hidden models are created using the sun-based PV display. The PV show's P-V quality under a sudden shift in insolation (for three guise models).

Three distinct disguise models are created at 0.2 s intervals to support the estimate. The P-V brand name has one GP under cover I at 38.36 W, cover II at 33.64 W, and shade-III at 26.47 W, as seen in Fig. 14. Fig. 15 mimics the PV system and displays a range of waveforms.

Shade-I is created at t = 0, cover II is created at t = 0.2 s, and shade-III is created at t = 0.4 s, as seen in Fig. 15(a). Under disguise I, the PV system with the WO estimate is ready to follow the maximum limit power of 37.06 W at t = 0.115 s. Verifying the try out findings provided by the conventional PO, GWO, and HGWO estimations supports the presentation of the WO computation. The GWO computation can be ready to follow 35.12 W, the PO estimation can follow 32.68 W, and the HGWO estimation can follow 36.65 W. PO, GWO, and HGWO have separate accompanying times of 0.189 s, 0.1459 s, and 0.1759 s. With the WO computation, the PV structure is ready to track the best power of 31.34 W at t = 0.0720 s under conceal II. Exclusively under conceal II, the PO, GWO, and HGWO may fit to follow 27.87 W, 30.42 W, and 31.12 W separately at 0.1698 s, 0.1178 s, and 0.1028 s. With WO calculation, the PV structure is ready to track the highest power of 24.71 W at t = 0.0850 s under conceal III.

Under Hide III, the PO, GWO, and HGWO are ready to follow 20.04 W, 22.14 W, and 23.86 W independently at 0.1598 s, 0.1278 s, and 0.1141 s. The PV display yield voltage and current are supporting waveforms, which essentially looks at the PV structure's introduction. The commitment cycle change under assault change in the isolation condition is depicted in Fig. 15(d). The ideal causes it to be seen that the commitment examples of WO, PO, GWO, and HGWO are, respectively, 0.2185, 0.4485, 0.3165, and 0.2082, at the concealed time of the estimates. Furthermore, it is observed that under rapidly changing isolation conditions, the traditional PO estimate attempts to track the GP (but fails to settle at GP), and the association time is longer than that of the suggested WO estimation and other computations such as GWO and HGWO. Since there are no extraordinary executives on the GWO or HGWO, as was previously noted, the likelihood of sliding into LP is increased. Because of the hybridization, the HGWO is ready to follow the best power, much like the WO estimate, because of the PO's going close to the GP. Given that the whales are resurrected, it is assumed that the WO computation tries to settle extraordinarily close to the GP.

5 Try IV: Absurd shift of brightness dependent on daylight

The absurd shift in insolation to see as the GP rather than the LPs supports the PV structure using the suggested WO MPPT technique. As seen in Fig. 16, the concealing models are based on the sun-based PV display. Fig. 17 illustrates the PV bunch's P-V nature under the absurd shift in isolation settings. In order to enable the calculation, four distinct disguising models were created at a 0.15 s stretch (next to conceal VI and shade-VII), as seen in Fig. 16. The various P-V brand names are displayed in Fig. 17. The P-V brand name contains one GP beneath cover IV at 40.65 W, conceal V at 20.49 W, and cover VI at 8.051 W, as seen in Fig. 17. At shade-VII and disguise IV, the GP is In Fig. 18, the PV system is replicated and a variety of waveforms are displayed. The shade-IV is created at t = 0, disguise V is created at t = 0.15 s, cover VI is created at 0.3 s, and shade VII is created at t = 0.5 s, as seen in Fig. 18(a). At t = 0.1246 s, under conceal IV, the PV structure with the WO computation can be ready to follow the most outrageous power of 40.53 W. It is possible to produce the PO estimate to follow 40.52 W, the GWO computation to follow 40.51 W, and the HGWO estimation to follow 40.53 W. The corresponding times for WO, PO, GWO, and HGWO are, respectively, 0.1246 s, 0.1515 s, 0.1248 s, and 0.1285 s.

Every calculation may be set up to essentially follow a similar MPP under STCs that have varying follow-up times. Under Hide V, the PV system with the WO estimate is ready to follow the best power of 16.41 W at t = 0.1209 s. Under cover V, the PO, GWO, and HGWO can only follow 11.87 W, 14.69 W, and 15.24 W at 0.1462 s, 0.1411 s, and 0.1396 s, respectively. With the WO computation, the PV structure is ready to track the highest power of 7.28 W at t = 0.1132 s under conceal VI. Under shadeVI alone, the PO, GWO, and HGWO are ready to follow 4.96 W, 6.11 W, and 7.91 W independently at 0.1478 s, 0.1411 s, and 0.1359 s. Similar to hide IV but with a different follow-up duration, hide VII offers the best power extraction. Under cover VII, the corresponding times for different estimates such as WO, PO, GWO, and HGWO are, respectively, 0.1246 s, 0.1549 s, 0.1252 s, and 0.1292 s. The PV display yield voltage and current are supporting waveforms in Fig. 18(b)–(c), which validates the PV system's presentation. The commitment cycle change under assault change in the isolation condition is depicted in Fig. 18(d). The ideal causes it to be seen that the commitment examples of WO, PO, GWO, and HGWO are, respectively, 0.3111, 0.4485, 0.3111, and 0.3263 during the fundamental period of the estimates. Furthermore, it is seen that the gathering time is longer than the suggested WO estimation and that the usual PO, GWO, and HGWO MPPT approach attempts to follow the GP (but fails to settle at GP) under the ludicrous change in insolation conditions. There is some evidence of influence in the PO method; similarly, this will generally be lessened by selecting a smaller step size, which will also lengthen the blend time. According to the previously conducted analysis, there is no outstanding director for the GWO or HGWO, and the likelihood of slipping into LP is almost 100% extended. Because of hybridization, the HGWO is ready to follow the best power, which is about equivalent to the WO estimate because of the PO's path close to the GP. Because the whales are re-energized and reinitialized in each stage separately to reduce the mix precision, the manner the WO computation attempts to settle makes it pondered to settle extremely nearer to the GP. Similar to high efficiency; (ii) entertainment tests are completed under various exams to assess the effectiveness of WO computation with diverse systems; and (iii) an execution examination pertaining to ML, FF, RPG, and RPL was distributed. In light of these conversations, the diving solicitation of the MPPT technique is, in addition to the PO technique, WO, HGWO, and GWO. By adhering to additional data constraints that are contingent on time and working conditions, the continuing task may be connected.

Furthermore, taking high trading repetition into consideration limits the work that has been completed on the lift converter in this research.

6 Examining the different MPPT methods under PSCs for execution

The goal of this portion of the research is to determine which MPPT system provides the highest working execution by examining the appraisal limitations of several MPPT methods, such as PO, GWO, HGWO, and the suggested WO computation under PSCs. The execution relationship for the 4S PV bunch game plans with the various concealment models is mostly determined by the following adequacy and association rate. Table 2 presents the assessment subtleties of productivity and following time. The graphical relationship between several MPPT techniques, such as WO, PO, GWO, and HGWO, is displayed. With respect to legitimate applications, the suggested WO MPPT approach is examined using standard estimations such as PO, GWO, and HGWO.

The previous explanations and Figs. 8–18 demonstrate that the WO technique discovers the GP precisely under various concealment models. In addition, the WO-based MPPT approach produces high MPPT after viability and a high intermixing rate. The last steps in the show examination are to register the fumbling incident (ML), relative influence setback (RPL), relative impact gain (RPG), fill factor (FF), and speculative power ages under various disguise settings. The rate is not fixed and is referred to as ΔPL. The most outrageous result is the power that different MPPT tactics under different disguise models transmit. The relationship between RPL and RPG across many MPPT approaches under distinct disguise models.

For a more thorough evaluation, the data names for the WO and HGWO processes. The S-VII hiding model is not taken into consideration for graphical connections as the S-IV and S-VII hiding models are relative.The outcome power and MPPT technique inside the PV systems are associated, as shown by the result obtained from the reenactment. The PV MPPT approaches are indicated similarly as RPL as follows: PO > GWO > GWO > WHO from, and similarly as RPG as follows: PO < GWO \ GWO \ WO. According to the reenactment findings, the WO MPPT method performs better than other MPPT systems, such as PO, GWO, and HGWO, since it has a higher effect gain and less influence mishap. Furthermore, the suggested method outperforms the PO, GWO, and HGWO in terms of following time, ML, FF, and following capability. In conclusion, the WO MPPT technique with reinitialization is ready to adapt to various working situations, such as STC, PSCs, rapid and extreme changes in solar radiation.

7 Conclusion

This work examined an additional MPPT approach that takes into account the WO calculation with reinitialization to adhere to the GP when the PV module is exposed to various covering models, such as P-I, PII, and S-I through S-VII. The introduction of the WO calculation and other estimates that affect the power age have been examined in this work. The WHO estimation's mathematical representation is complete, and the WO computation's implementation for the MPPT application is fully understood. The automated experience concluded in favor of the suggested strategy's introduction. The suggested method is supported by 4S PV display configurations in a variety of disguising scenarios, including STCs, PSCs, abrupt changes in insolation, and ludicrous variations in insolation. The constraints such as most prominent power extraction, following time, following efficiency, ML, FF, RPG, and RPL are taken into consideration while reviewing the MPPT techniques displayed. It is concluded from the well-organized reenactment and conversations that the suggested approach has high viability and is common in requiring less time and influencing setbacks. To reduce the calculation weight of the WO estimation, 12 mission specialists with 100 emphases were selected for the diversion evaluation. Lastly, the suggested MPPT approach has a lower standard deviation, which makes it possible to discover the GP more successfully and conclusively. The crucial responsibilities of this work are as follows: (I) demonstrating and implementing an additional MPPT application to follow the GP with less power influencing and less following time.

References

1. R. Abdul-Kalaam, S. Muyeen, A. Al-Durra. *Review of maximum power point tracking techniques for photovoltaic system.* Glob. J. Control Eng. Technol, **2**, 8-18, (2016)
2. K. Ahmad El, A.R. Nasrudin, S. Jeyraj, M. NasirUddin.*Fuzzy logic controller-based SEPIC converter for maximum power point tracking.* IEEE Trans. Ind. Appl. **50,** 4, 2349–2358, (2014)
3. J. Ahmed, Z. Salam. *A critical evaluation on maximum power point tracking methods for partial shading in PV systems.* Renew. Sustain. Energy Rev. **47**, 933–953, (2015)
4. A. Badis, M.N. Mansouri, M.H. Boujmil.*A genetic algorithm optimized MPPT controller for a PV system with DC-DC boost converter*. In: Proc. of International Conference on Engineering &, Monastir, 1-6, (2017)

5. M. Bahrami, M. Zandi, R. Gavagsaz, B. Nahid-Mobarakeh, S. Pierfederici. *A new hybrid method of MPPT for photovoltaic systems based on FLC and three point-weight methods.* In IEEE 7th Power Electronics and Drive Systems Technologies Conference (PEDSTC), 446-450, (2016)
6. F. Belhachat, C. Larbes. *Comprehensive review on global maximum power point tracking techniques for PV systems subjected to partial shading conditions.* Sol. Energy **183**, 476–500, (2019)
7. H. Bellia, R. Youcef, M. Fatima. *A detailed modeling of photovoltaic module using MATLAB.* NRIAG J. Astron. Geophys. **3**, 1, 53–61, (2014)
8. A.S. Benyoucefa, A. Chouderb, K. Karaa, S. Silvestrec, O.A. Sahedaa. *Artificial bee colony-based algorithm for maximum power point tracking (MPPT) for PV systems operating under partial shaded conditions.* Appl. Soft Comput. **32**, 38–48, (2015)
9. H.u. Chao, W. Long, L. Huan, L. Xiong, W. Jenq-Haur. *A hybrid global maximum power point tracking method for photovoltaic arrays under partial shading conditions.*Optik Int. J. Light Electron Opt.,**180**, 665–674, (2019)
10. El-Khozondar, J. Hala El-Khozondar, J. Rifa Matter, Khaled, Suntio, Teuvo. *A review study of photovoltaic array maximum power tracking algorithms.* Renewables,**3,** 3, 1–8, (2016).
11. Farh, M.H. Hassan Eltamaly, M. Ali Othman, F. Mohd. *Hybrid PSO-FLC for dynamic global peak extraction of the partially shaded photovoltaic system.*PLoS One **13**, 11, (2018)
12. I. Haidar, S. Mekhilef, N.B. Mohamed Shah, T.K. Soon, M. Seyedmahmousian, B. Horan, A. Stojcevski. *Performance evaluation of maximum power point tracking approaches and photovoltaic systems.* Energies,**11**, (2018)
13. C. Huang, L. Wang, R.S.C. Yeung, Z. Zhang, H.S.H. Chung, A. Bensoussan. *A prediction model-guided jaya algorithm for the PV system maximum power point tracking.* IEEE Trans. Sustain. Energy,**9**, 1, 45–55, (2018)
14. S. Ji-Ying, X. Fei, Q. Zi-Jian, Z. Wen, L. Le-Tao, Y. Ting. *Improved global maximum power point tracking for photovoltaic system via cuckoo search under partial shaded conditions.* J. Power Electron. **16**, 1, 287–296, (2016)
15. L.L. Jiang, D.R. Nayanasiri, Maskell, L. Douglas D.M. Vilathgamuwa. *A hybrid maximum power point tracking for partially shaded photovoltaic systems in the tropics.* Renew. Energy,**76**, 53–65, (2015)
16. Karami, Nabil, Moubayed, Nazih, Outbib, Rachid. *General review and classification of different MPPT techniques.*Energy Rev.,**68**, 1, 1–18, (2017)
17. M. Kermadi, E.M. Berkouk. *Artificial intelligence-based maximum power point tracking controllers for photovoltaic systems: Comparative study.* Renew. Sustain. Energy Rev.,**69**, 369–386, (2017)
18. T. Kok Soon, M. Saad, Y. Hong-Tzer, C. Ming-Kai. *A differential evolution based MPPT method for photovoltaic modules under partial shading conditions.* Int. J. Photoenergy,**2014**, 1-10, (2014)
19. S. Madeti, S. Singh. *Comparative analysis of solar photovoltaic monitoring systems.* AIP Conf. Proc.,**1859**, 1–6, (2017)
20. S. Mirjalili, A. Lewis. *The whale optimization algorithm.* Adv. Eng. Softw.,**95**, 51–67, (2016)
21. S. Mohanty, B. Subudhi, P.K. Ray. *A grey wolf-assisted perturb & observe MPPT algorithm for a PV system.* IEEE Trans. Energy Convers.,**32**, 1, 340–347, (2017)

22. S. Mohanty, B. Subudhi, P.K. Rey. A *new MPPT design using gray wolf optimization techniques for photovoltaic systems under partial shading conditions.* IEEE Trans. Sustain. Energy.,**7**, 1, 181–188, (2016)
23. B. Peng, K. Ho, Y. Liu. *A novel and fast MPPT method suitable for both fast changing and partially shaded conditions.* IEEE Trans. Ind. Electron.,**65,** 4, 3240–3251, (2018)
24. M. Premkumar, K. Karthick, R. Sowmya. *A comparative study and analysis on conventional solar PV based DC-DC converters and MPPT techniques.*Indones. J. Electr. Eng. Comput. Sci.,**11**, 3, 831–838, (2018).
25. M. Premkumar, R. Sowmya. *Certain study on MPPT algorithms to track the global MPP under partial shading on solar PV module/array.* Int. J. Comput. Digit. Syst.,**8**, 4, 405–416, (2019).
26. M. Penconi, G. Bianchi, A. Nitti, A. Savoini, C. Carbonera, D. Pasini, R. Po, S. Luzzati*A Contributor Polymer with a Decent Split the difference among Proficiency and Manageability for Natural Sunlight based Cells.* Adv. Energy Support. Res.,(2021)
27. I. Etier, A. Al Tarabsheh, N. Kannan. Shunt resistance spatial variations in amorphous silicon solar cells. Microelectron. J., **108**, (2021)
28. I.S. Millah, R.K. Subroto, Y.W. Chang, K.L. Lian, B.R. Ke.*Examination of Greatest Power Point Following of Various types ofSunlight powered chargers Under Halfway Concealing Circumstances.* IEEE Trans. Ind. Appl., **57**, 17-25,(2021)
29. A. Chen, M. Yossef, C. Zhang. *Strain effect on the performance of amorphous silicon and perovskite solar cells.* Solar Energy, **163**, 243-250, (2018).
30. V M Revathi et al, "A modified invasive weed optimization for MPPT of PV based water pumping system driven by induction motor, IOP: Engineering Research Express, volume 6, number 3, July 2024, 10.1088/2631-8695/ad5cd3.
31. Kandi Bhanu Prakash, Suresh Kakinatla, Sankara Rao Burada and Siva Ganesh Malla, "Hybrid Renewable Energy Sources based Mobile Charging Unit for Public Usage", 1st International Conference on Power and Energy Systems (ICPES 2023), E3S Web of Conf, Volume 540, June 2024, https://doi.org/10.1051/e3sconf/202454001001.
32. Priyanka Malla, "Novel Control Technique for MPPT of PV Standalone System with TSK Fuzzy controller", International Journal of New Technologies in Science and Engineering (IJNTSE), Vol. 8, Issue. 8, pp. 1-7, Aug. 2022.
33. Malla, Priyanka, Malla, Siva Ganesh and Calay, Rajnish Kaur. "Voltage control of standalone photovoltaic – electrolyzer- fuel cell-battery energy system" International Journal of Emerging Electric Power Systems, vol. 24, no. 5, 2023, pp. 649-658. https://doi.org/10.1515/ijeeps-2022-0047.
34. M. Panda, O. Al Zaabi, K. Al Jaafari, P. Kumar, K. Al Hosani and U. R. Muduli, "State-of-Charge Droop Control for Efficient Power Sharing and Transient Response in Microgrids," 2023 IEEE IAS Global Conference on Emerging Technologies (GlobConET), London, United Kingdom, 2023, pp. 1-5, doi: 10.1109/GlobConET56651.2023.10149905.
35. R. K. Meena, D. V. Bhaskar, O. Al Zaabi, M. Panda, P. Kumar and U. R. Muduli, "Modeling of Two-Stage Photovoltaic Inverter with Grid Connected and Islanding Operation," 2023 IEEE IAS Global Conference on Renewable Energy and Hydrogen Technologies (GlobConHT), Male, Maldives, 2023, pp. 1-6, doi: 10.1109/GlobConHT56829.2023.10087517.
36. N. Chaudhary, A. Ranjan, D. V. Bhaskar, M. Panda, A. Kumar and P. Kumar, "Harmonic Reduction Strategies for EV Charging in Power Systems Using Shunt Active Power Filter," 2023 3rd International Conference on Emerging Frontiers in Electrical and Electronic Technologies (ICEFEET), Patna, India, 2023, pp. 1-6, doi: 10.1109/ICEFEET59656.2023.10452228.

37. S. K. Baksi, R. K. Behera and U. R. Muduli, "Optimized 9-Level Switched-Capacitor Inverter for Grid-Connected Photovoltaic Systems," in IEEE Transactions on Industry Applications, vol. 60, no. 2, pp. 3284-3296, March-April 2024, doi: 10.1109/TIA.2023.3332059.
38. Kandi Bhanu Prakash, "PV-Battery based standalone power supply system for rural applications", International Journal of New Technologies in Science and Engineering (IJNTSE), Vol. 8, Issue. 12, pp. 9-13, Dec. 2022.
39. A. Saxena et al., "Intelligent Load Forecasting and Renewable Energy Integration for Enhanced Grid Reliability," in IEEE Transactions on Industry Applications, doi: 10.1109/TIA.2024.3436471.
40. Pragathi, B., Poonia, R.C., Polaiah, B. et al. Evaluation and Analysis of Soft Computing Techniques for Grid Connected Photo Voltaic System to Enhance Power Quality Issues. J. Electr. Eng. Technol. 16, 1833–1840 (2021). https://doi.org/10.1007/s42835-021-00720-w.
41. Pamula Raja Kumari and Polaiah Bojja and B. Pragathi and T Prasanth kumar reddy and P Vijaya Lakshmi, Evaluation and Implementation of Particle Swarm Optimization Maximumpower Point Tracking Technique for Photo Voltaic System, Journal of Physics: Conference Series, Vol 1804, Feb 2021, https://dx.doi.org/10.1088/1742-6596/1804/1/012188.